0026-895X/09/7504-982–990$20.00
MOLECULAR PHARMACOLOGY
Copyright © 2009 The American Society for Pharmacology and Experimental Therapeutics
Mol Pharmacol 75:982–990, 2009

Vol. 75, No. 4
53686/3455165
Printed in U.S.A.

Conformational Toggle Switches Implicated in Basal Constitutive and Agonist-Induced Activated States of 5-Hydroxytryptamine-4 Receptors

Lucie P. Pellissier, Jessica Sallander, Mercedes Campillo, Florence Gaven, Emilie Queffeulou, Marion Pillot, Aline Dumuis, Sylvie Claeysen, Joël Bockaert, and Leonardo Pardo

Centre National de la Recherche Scientifique Unité Mixte de Recherche 5203, Institut de Génomique Fonctionnelle, Institut National de la Santé et de la Recherche Médicale U661, Universités Montpellier 1 and 2, Montpellier, France (L.P.P., F.G., E.Q., M.P., A.D., S.C., J.B.); and Laboratori de Medicina Computacional, Unitat de Bioestadística, Facultat de Medicina, Universitat Autònoma de Barcelona, Bellaterra, Spain (J.S., M.C., L.P.)

Received November 27, 2008; accepted January 22, 2009

ABSTRACT

The extended classic ternary complex model predicts that a G protein-coupled receptor (GPCR) exists in only two interconvertible states: an inactive R, and an active R*. However, different structural active R* complexes may exist in addition to a silent inactive R ground state (Rg). Here we demonstrate, in a cellular context, that several R* states of 5-hydroxytryptamine-4 (5-HT_4) receptors involve different side-chain conformational toggle switches. Using site-directed mutagenesis and molecular modeling approaches, we show that the basal constitutive receptor (R*basal) results from stabilization of an obligatory double toggle switch (Thr3.36 from inactive *g*− to active *g*+ and Trp6.48 from inactive *g*+ to active *t*). Mutation of either threonine or tryptophan to alanine resulted in a lowering of the activity of the R*basal similar to the Rg. The T3.36A mutation shows that the Thr3.36 toggle switch plays a minor role in the stabilization of R* induced by 5-HT (R*-5-HT) and BIMU8 (R*-BIMU8) and is fully required in the stabilization of R* induced by (*S*)-zacopride, cisapride, and 1-(4-amino-5-chloro-2-methoxyphenyl)-3-(1-butyl-4-piperidinyl)-1-propanone (RS 67333) (R*-benzamides). Thus, benzamides stabilize R*-benzamides by forming a specific hydrogen bond with Thr3.36 in the active *g*+ conformation. Conversely, R*-BIMU8 was probably the result of a direct conformational transition of Trp6.48 from inactive *g*+ to active *t* by hydrogen bonding of this residue to a carboxyl group of BIMU8. We were surprised that the Trp6.48 toggle switch was not necessary for receptor activation by the natural agonist 5-HT. R*-5-HT is probably attained through other routes of activation. Thus, different conformational arrangements occur during stabilization of R*basal, R*-5-HT, R*-benzamides, and R*-BIMU8.

G protein-coupled receptors (GPCRs) are allosteric molecules in equilibrium with many different conformational states (Samama et al., 1993; Bond et al., 1995). GPCRs adopt at least one inactive (R) and several active (R*) states (Ghanouni et al., 2001; Okada et al., 2001; Alves et al., 2003; Swaminath et al., 2004; Baneres et al., 2005). R* states can be reached, even in the absence of agonists or mutations (called here basal constitutively active R* or R*basal), whereas chemically different ligands can stabilize different R* states. Partial agonists may stabilize a specific receptor state different from the R* of full agonist. For example, using circular dichroism difference spectra of the purified 5-HT_4 receptor, we have previously found that free (or neutral antagonist-occupied), agonist-occupied (partial or full agonist),

This work was supported by the Centre National de la Recherche Scientifique; Institut National de la Santé et de la Recherche Médicale; Ministère Français de la Recherche [Grant ANR Blanc-2006-0087-02]; Université de Montpellier; Ministerio de Educación y Ciencia [Grants SAF2006-04966, SAF-2007-67008]; and Instituto de Salud Carlos III [RD07/0067/0008]. Binding experiments, cAMP measurement, and ELISA were carried out using facilities of the Pharmacological Screening platform of the Institut de Génomique Fonctionnelle.

L.P.P. and J.S. equally contributed to this work.

Article, publication date, and citation information can be found at http://molpharm.aspetjournals.org.
doi:10.1124/mol.108.053686.

ABBREVIATIONS: GPCRs, G protein-coupled receptors; 5-HT, 5-hydroxytryptamine; 5-HT_4R, 5-hydroxytryptamine-4 receptor; Rg, inactive R ground state; TM, transmembrane; HA, hemagglutinin; ELISA, enzyme-linked immunosorbent assay; WT, wild type; BIMU8, *N*- [(1*R*,5*S*)-8-methyl-8-azabicyclo[3.2.1]oct-3-yl]-2,3-dihydro-3-iso-propyl-2-oxo-1*H*-benzimidazol-1-carboxamide hydrochloride; (*S*)-zacopride, (*S*)-*N*-(1-azabicyclo-[2.2.2]oct-3-yl)-4-amino-5-chloro-2-methoxybenzamide monohydrochloride; cisapride, *cis*-4-amino-5-chloro-*N*-{1-[3-(4-fluoro-phenoxy)propyl]-3-methoxy-4-piperidinyl}-2-methoxy benzamide; RS 67333, 1-(4-amino-5-chloro-2-methoxy-phenyl)-3-(1-butyl-4-piperidinyl)-1-propanone; RO 116-1148 2,3-dihydrobenzo-(1,4)-dioxine-5-carboxylic acid 1-butylpiperidin-4-ylmethylamide hydrochloride; GR 113808, 1-methyl-1*H*-indole-3-carboxylic acid [1–2-[(methyl sulfonyl) amino] ethyl-4-piperidinyl] methyl ester; CSP-2503, 2-((4-(naphth-1-yl)piperazin-1-yl)methyl)-1,4-dioxoperhydropyrrolo(1,2-*a*)pyrazine.

and silent (inverse agonist-occupied) receptors involved different arrangement of the e_2 loop (Baneres et al., 2005). Inactive R state of family A GPCRs is generally not the equivalent to the "silent" state of the *cis*-retinal-rhodopsin receptor complex called the ground state (Rg) (Palczewski et al., 2000; Park et al., 2008). Recent insights into the β_2-adrenergic receptor structure indicate that even in the presence of the partial inverse agonist carazolol, this receptor is certainly not under the Rg state and adopts a structural feature of the R* states (a relatively open "ionic lock") (Cherezov et al., 2007; Rosenbaum et al., 2007). Therefore, the Rg state may only be reached with full inverse agonists such as the *cis*-retinal and the R state may be, in some receptors, already an R* (Palczewski et al., 2000).

One of the main questions in GPCR molecular pharmacology is to understand the structural arrangements of the seven transmembrane (TM) helices that occur to stabilize either Rg or the different R* states. It is noteworthy that some main arrangement and rearrangement events during activation seem to be common, at least in family A GPCRs (Ruprecht et al., 2004; Schertler, 2005; Kobilka, 2007; Smit et al., 2007).

The recent crystal structure of the ligand-free opsin, which contains several features characteristic of R* states (Park et al., 2008), has shown that the intracellular part of TM6 is tilted outward by 6 to 7 Å, whereas TM5 moves toward TM6 by 2 to 3 Å. In addition, conformational changes occurring to generate either Rg or R* states are accomplished by the rearrangement of side chains forming different networks of interactions between helices (Shi et al., 2002; Rosenbaum et al., 2007; Smit et al., 2007). The structure of metarhodopsin I by electron crystallography (Ruprecht et al., 2004; Schertler, 2005), experimental studies of rhodopsin (Lin and Sakmar, 1996), and computer simulations associated with mutagenesis of β_2-adrenergic (Shi et al., 2002), 5-HT$_{2A}$ (Visiers et al., 2002), cannabinoid 1 (McAllister et al., 2004), and histamine H_1 receptors (Jongejan et al., 2005) have shown that Trp6.48 of the conserved CWxPFF motif of TM6 undergoes a conformational transition, from pointing toward TM7 in the inactive state to pointing toward TM5 in the agonist-induced R* (Ruprecht et al., 2004; Schertler, 2005). The side chain at position 3.36 has also been suggested to act as a rotamer toggle switch simultaneously with Trp6.48 in the histamine H_1 and cannabinoid 1 receptors (McAllister et al., 2004; Jongejan et al., 2005).

In this study, we have investigated the 5-HT$_4$ receptor (5-HT$_4$R) and its ability to stabilize different R* states. The focus was mainly put on the roles of the Trp6.48 rotamer toggle switch and its associated toggle switch at position 3.36. We found that both toggle switches were required for stabilizing the basal R* state (called R*basal), none of them were fully implicated in stabilizing the R* reached in the presence of 5-HT (called R*-5-HT), whereas the Thr3.36 and the Trp6.48 toggle switches were implicated in stabilizing the R* in the presence of synthetic agonists belonging to either the benzamide or aryl ketone classes (called R*-benzamides), or to a benzimidazolone class (called R*-BIMU8).

Materials and Methods

Plasmid Construct. HA-tagged-5-HT$_4$ receptor cDNAs in pRK5 were generated by fusing the sequence of the HA epitope (YPYDVPDYA) to a cleavable signal peptide (MVLLLILSVLLLKEDVRGSAQS) derived from the metabotropic glutamate receptor 5. This sequence was inserted into the pRK5 vector using XbaI and BsrGI restriction sites. Then, full-length mouse 5-HT$_{4(a)}$R cDNAs were subcloned in frame using BsrGI and Hind III. HA-5-HT$_4$-T3.36A, HA-5-HT$_4$-T3.36S, HA-5-HT$_4$-T3.36C, and HA-5-HT$_4$-W6.48A receptor mutants were generated from HA-5-HT$_{4(a)}$R, cloned in pRK5 with the QuikChange Site-Directed Mutagenesis Kit (Stratagene, Amsterdam, the Netherlands).

Membrane Preparation and Radioligand Binding Assay. Membranes were prepared from transiently transfected cells plated on 15-cm dishes and grown in Dulbecco's modified Eagle's medium with 10% dialyzed fetal calf serum as described by Claeysen et al. (2003). The membrane solubilized in 50 mM HEPES, pH 7.4 (5 mg of protein in 1 ml of solution), were stored at −80°C until use. Membrane suspension (approximately 10 μg), diluted in 100 μl of 50 mM HEPES containing 10 mM pargyline and 0.01% ascorbic acid, was incubated at 20°C for 30 min with 100 μl of [^{3}H]GR 113808 (specific activity, 82 Ci/mmol) and 50 μl of buffer or competing drugs. For saturation analysis assays, various concentrations of [^{3}H]GR 113808 (0.001–0.8 nM) were used. BIMU8 (10 μM) was used to determine nonspecific binding. Protein concentration was determined by using the bicinchoninic acidic method.

Cell Surface ELISA. COS-7 cells were transfected with HA-tagged 5-HT$_4$R, WT, or mutant cDNAs. Cells were grown on 96-well plates in Dulbecco's modified Eagle's medium with 10% dialyzed fetal calf serum and fixed as described previously (Barthet et al., 2005). Cells were then incubated with anti-HA antibody at 0.6 μg/ml for 60 min in the same buffer and incubated with anti-rabbit/horseradish peroxidase conjugate (GE Healthcare, Chalfont St. Giles, Buckinghamshire, UK) at 1 μg/ml for 60 min. Chromogenic substrate was added (Supersignal ELISA femto-maximum sensitivity; Pierce, Perbio-Brebières, France). Chemiluminescence was detected and quantified by a Wallac Victor^2 luminescence counter (PerkinElmer Wallac, Gaithersburg, MD).

Determination of cAMP Production in Transfected Cells. COS-7 cells were transfected with the appropriate cDNA and seeded into 24-well plates (100,000 cells/well). 24 h after transfection, a 10-min stimulation with the appropriate concentrations of drugs was performed as described previously (Barthet et al., 2005). Quantification of cAMP production was performed by Homogenous Time Resolved Fluorescence using the cAMP Dynamic kit (Cisbio International, Bagnols-sur-Cèze, France) according to the manufacturer's instructions.

Data Analysis. The dose-response curves were fitted using Prism software (GraphPad Software Inc., San Diego, CA) and the following equation for monophasic dose-response curves: $y = (y_{max} - y_{min})/1 + [(x/EC_{50})\ n_H] + y_{min}$, where EC_{50} is the concentration of the compound necessary to obtain 50% of the maximal effect, and n_H is the Hill coefficient. Competition and saturation experiments were analyzed by nonlinear regression using GraphPad Prism as described previously (Ansanay et al., 1996). All data represented correspond to the mean ± S.E.M. of three independent experiments performed in triplicate. Statistical analysis was carried out with the *t* test using GraphPad Prism 3.0 software.

Nomenclature of Side Chain Conformation. The side chain conformation has been categorized into *gauche*− (*g*−: 0° < χ_1 < 120°), *trans* (*t*: 120° < χ_1 < 240°), or *gauche*+ (*g*+: 240° < χ_1 < 360°) depending on the value of the torsional χ_1 angle.

Numbering Scheme of GPCRs. Residues are identified by the generic numbering scheme of Ballesteros and Weinstein (1995) that allows easy comparison among residues in the 7TM segments of different receptors.

Computational Model of the Ligand-Receptor Complexes. A model of the 5-HT$_4$R was constructed by homology modeling using the crystal structure of the β_2-adrenergic receptor (Protein Data Bank code 2RH1) (Cherezov et al., 2007; Rosenbaum et al., 2007) as template. The 5-HT, BIMU8, and (*S*)-zacopride ligands were docked by interactive computer graphics into the receptor model with their

protonated side chain interacting with Asp3.32 in TM3 (Shi and Javitch, 2002). The Duan et al. (2003) force field was used for peptides, and the general Amber force field (Wang et al., 2004) and HF/6–31G*-derived RESP atomic charges were used for the ligands. In an explicit lipidic bilayer, molecular dynamics simulations of the ligand-receptor complexes were performed with the Sander module of AMBER 9 (Case et al., 2006) using the protocol described previously (Jongejan et al., 2005).

Drugs. The following compounds were used: BIMU8, (*S*)-zacopride, cisapride, RS 67333, and RO 116-1148.

Results

The Role of Thr3.36 and Trp6.48 in Stabilizing the Basal Constitutive Activity of 5-HT$_4$ Receptors (R*basal). We have previously shown that the constitutive activity of the histamine H_1 receptor was dependent on the nature of the residue at position 3.36 (Jongejan et al., 2005). When serine, present in the WT H_1 receptor, was substituted by threonine or cysteine, the basal constitutive activity increased dramatically, occluding the histamine activation, whereas the constitutive activity was nonexistent when serine was substituted by alanine. In biogenic amine receptors, the 3.36 position is rarely occupied by threonine (1%) and more often by cysteine (56%) or serine (31%). It is noteworthy that position 3.36 is occupied by threonine in 5-HT$_4$Rs. This may explain why 5-HT$_4$Rs have such a high constitutive activity. We engineered the T3.36A/S/C mutant receptors to study the role of the short and polar side chain of Thr3.36 in the constitutive activity of the 5-HT$_4$R. By using different plasmid concentrations, we managed to obtain similar cell surface expression of the WT 5-HT$_4$R and T3.36A/S/C mutants. This was confirmed by using an ELISA assay (Fig. 1A) but also by Scatchard analysis using the specific labeled 5-HT$_4$R ligand [^{3}H]GR 113808, as described previously (Claeysen et al., 1999) (Fig. 1A). The T3.36A mutation almost abolished the constitutive activity (Fig. 1B), indicating that the hydrogen bond capability of Thr3.36 plays an important role in stabilizing R* adopted by constitutively active 5-HT$_4$Rs. T3.36S/C mutations provide a way of identifying the conformation of Thr3.36 in the active state of the R*basal because of the different side chain rotamer distribution of threonine from those of serine or cysteine when located in an α-helical structure (Fig. 1C) (Ballesteros et al., 2000). The conformations of the short and β-branched side chain of threonine are limited to the $g+$ (85% of the side chains) and $g-$ (15%) because the t conformation is unfavorable because of the steric clash of the side chain methyl group with the backbone carbonyl at the i-3 position (McGregor et al., 1987). In contrast, serine can adopt either the $g+$ (52%), $g-$ (20%), or t (28%) rotamer conformation. The fact that T3.36S reduces the constitutive activity of the receptor to a level close to the value observed in the T3.36A mutation precludes the serine-specific t conformation as the active conformation. Cysteine is restricted to the $g+$ (71%) or t (29%) conformation because of the steric clash between the Sγ atom and the carbonyl oxygen of residue i-3 in the $g-$ conformation (McGregor et al., 1987). The unchanged constitutive activity of the T3.36C mutation, relative to WT, points to the common $g+$ conformation of cysteine and threonine as the active conformation, in agreement with previous proposals (Jongejan et al., 2005). We thus propose that Thr3.36 in the 5-HT$_4$R undergoes a conformational transition from the inactive $g-$ to the active (R*basal) $g+$ conformation. Molecular modeling showed that this conformational transition is only feasible if the side chain of Trp6.48 modifies its conformation simultaneously, in a concerted manner, from the inactive $g+$ to the active t conformation (Fig. 1D). Both the Trp6.48 and the Thr3.36 concerted toggle switches were absolutely necessary to adopt the R* constitutive active state (R*basal). Indeed, as described previously, the W6.48A mutant (Joubert et al., 2002) as well as the T3.36A mutant were under the Rg state (Fig. 1B).

To be certain that both mutations (T3.36A and W6.48A) were stabilizing the 5-HT$_4$R under an Rg state, we studied the activities of these mutants as a function of the receptor density. As seen in Fig. 2A, the basal activity of the WT receptor increased proportionally to the plasmid concentration and up to 31 pmol/mg, whereas the basal activity of both T3.36A and W6.48A mutants remained totally in the Rg state whatever the receptor density (Fig. 2A). As expected, the inverse agonist RO 116-1148 had no effect on the basal activity in both W6.48A (Joubert et al., 2002) and T3.36A mutants, whereas it totally blocked the basal activity of the WT receptor (Fig. 2B). In conclusion, both the Thr3.36 and the Trp6.48 toggle switches were necessary to reach an R*basal.

Reaching the Maximal R*-5-HT State Does Not Require the Trp6.48 Toggle Switch, whereas the Thr3.36 Toggle Switch Is Partially Involved. When measured at similar cell surface density, the maximal activity (E_{max}) of

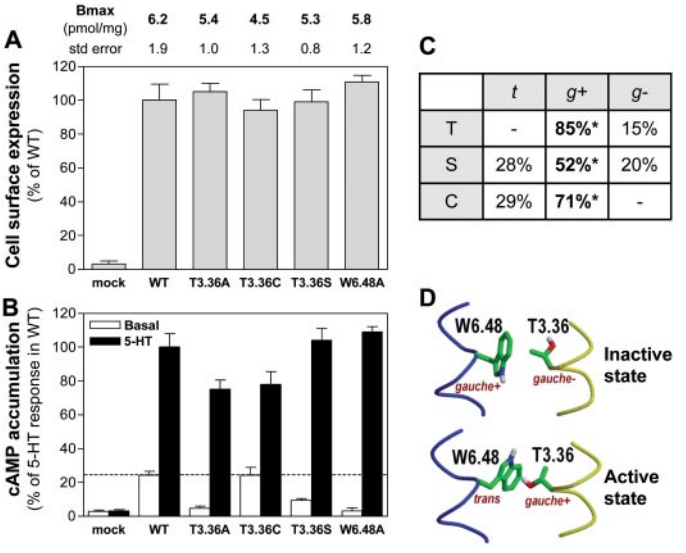

Fig. 1. Constitutive activity of the WT 5-HT$_4$R is largely dependent on Thr3.36. A, native and mutant receptors (5-HT4R-T3.36A/C/S-W6.48A) were transiently expressed in COS-7 cells. Expression receptor levels at the plasma membrane relative to the expression of the WT were determined by ELISA assay. The relative expression levels, indicated above the graph, expressed in femtomoles per milligram of protein, were for WT (6160 ± 1860), T3.36A (5390 ± 1010), T3.36C (4520 ± 1300), T3.36S (5300 ± 750), and Trp6.48 (5810 ± 1230). B, basal level and maximum 5-HT (10^{-5} M) stimulation of cAMP formation were measured after 10-min incubation. Each value was estimated as the percentage of maximum cAMP production (8.9 ± 0.7 pmol/100,000 cells) in the WT induced by 5-HT (10^{-5} M). C, statistical preferences of threonine (T), serine (S), and cysteine (C) side chain rotamer distribution (t, trans; $g+$, gauche+; or $g-$, gauche−; see *Materials and Methods*) when located in a α-helical structure (adapted from Ballesteros et al., 2000). Active conformations in the 5-HT4R are shown in boldface type and are indicated with an asterisk. D, 5-HT4R activation consists of a concerted Thr3.36/Trp6.48 rotamer toggle switch. Thr3.36 undergoes a conformational transition from the inactive $g-$ to the active $g+$ conformation, in conjunction with the conformational transition of Trp6.48 from the inactive $g+$ to the active t conformation.

the R*-5-HT state in WT and W6.48A mutant were not different (Fig. 1B and Table 1). In the Trp6.48 mutant, the EC_{50} value was shifted to the right by a factor of 25, despite the fact that the binding affinity of 5-HT for the W6.48A mutant receptor remained the same. Thus, the mutation did not affect 5-HT binding, weakly affected the coupling, and did not at all affect the maximal activity of the R*-5-HT state. In contrast, when measured at similar cell surface density, the maximal activity (E_{max}) of the R*-5-HT state in the T3.36A mutant decreased by 26% compared with that of the WT, whereas its EC_{50} value shifted to the right by a factor of 24, and its binding affinity was also reduced by a factor of 18. We constructed a three-dimensional model of the complex between 5-HT and a β_2-adrenergic receptor-based model of the 5-HT$_4$R (see *Materials and Methods*). This computational model considers that agonists bind the active conformation of the 5-HT$_4$R, in which Thr3.36 is pointing toward TM7 in the active $g+$ conformation and Trp6.48 is pointing toward TM5 in the active t conformation. The conformation of Phe6.52 was also modeled in t to avoid the steric clash with Trp6.48 (Shi et al., 2002). Thr3.36 in $g+$ participates, in addition to the known aspartic acid Asp3.32 in TM3, in the binding of the protonated amine of serotonin, which is similar to what has been described for histamine binding to the H_1 receptor (Jongejan et al., 2005). The indole ring of 5-HT expands toward TMs 5 and 6 to hydrogen bond the key Ser5.43 and Asn6.55 side chains (Fig. 5A), as proposed by site-directed mutagenesis (Mialet et al., 2000), without forming a direct interaction with Trp6.48. This mode of binding explains the fact that T3.36A slightly influences both the binding affinity for 5-HT and R*-5-HT (E_{max} and EC_{50} values) and that W6.48A does not modify the binding affinity or E_{max} value. Thus, the Trp6.48 toggle switch is not necessary to reach the R*-5-HT, whereas the T3.36 switch is only partially necessary. R*-5-HT is probably attained through other routes of activation involving TMs 5 and 6 (see *Discussion*).

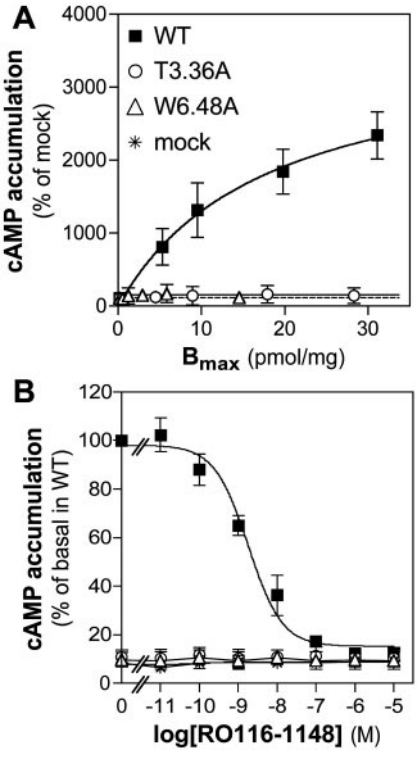

Fig. 2. Lack of basal activity and inverse agonist RO 116-1148 effect in T3.36A and W6.48A mutants. A, the relationship between receptor density and basal activity was measured in COS-7 cells expressing increasing density of WT, T3.36A, and W6.48A. cAMP production was expressed as a percentage over basal cAMP produced in the mock-transfected cells (0.13 ± 0.03 pmol/100,000 cells). B, the inverse agonist activity of RO 116-1148 was tested relative to basal constitutive cAMP production in WT, T3.36A, and W6.48A. The inverse agonist effect is represented as the percentage of basal cAMP formation taken as 100% (2.86 ± 0. 15 pmol/100,000 cells for 200 ng of WT 5-HT$_4$R cDNA transfected). Each value represents the mean ± S.E.M. determined from three independent experiments performed in triplicate.

The R*-Benzamide State Is Reached after a Direct Interaction of Benzamides with Thr3.36, Triggering Its Toggle Switch from the $g-$ to the $g+$ Conformation. It is noteworthy that the T3.36A mutation modified the process of receptor activation in an agonist-specific dependent manner (Table 1 and Fig. 3B). At similar receptor expression density, the E_{max} of the R*-BIMU8 state was weakly decreased by this mutation, from 97 to 78%, whereas the EC_{50} value was unchanged (Fig. 3 and Table 1). In contrast, activation by 2-methoxy-4-amino-5-chloro benzamides [(*S*)-zacopride, cisapride] and related aryl ketone (RS 67333) was almost eliminated (Fig. 3B and Table 1). It is noteworthy that cell surface expression of this T3.36A mutant was similar to that of the WT (Fig. 1A), and the lack of stimulation was not due to a loss of binding affinity of these ligands for the 5-HT$_4$R-T3.36A mutant (Table 1). Because the benzamides are partial agonists on the WT receptor, it was possible that a weaker coupling efficiency due to mutation could have a higher influence on the E_{max} of benzamides compared with that of WT. Therefore, we studied the influence of receptor density on the stimulation of 5-HT$_4$R by 5-HT, (*S*)-zacopride, and BIMU8 in WT and T3.36A mutant (Fig. 4). We have previously shown that, in COS-7 cells (Claeysen et al., 2000), the 5-HT$_4$R activation can be analyzed by the two-state model proposed by Leff (1995). In particular, the E_{max} value increased as the function of receptor density, but the EC_{50} value remains identical. This was again observed here when the dose-activation curves were determined on WT 5-HT$_4$R (Fig. 4, left). The 5-HT and BIMU8 dose-response curves determined on the T3.36A mutant also showed an increase in E_{max} value without change in EC_{50} value when the receptor density increased (Fig. 4, D and F). In contrast, the benzamide (*S*)-zacopride was totally unable to stimulate the T3.36A mutant whatever the receptor density (Fig. 4E and Table 1).

To propose a structural hypothesis of the small effect of the T3.36A mutation on activity of the R*-BIMU8 state and the specific elimination of the R*-benzamide state, we propose a model in Fig. 5, B and C, describing the complexes between these ligands and the 5-HT$_4$R. In addition to other pharmacophoric elements (Fig. 5), (*S*)-zacopride and BIMU8 contain key carbonyl groups that point toward TM3 (Fig. 5B) and TM6 (Fig. 5C), respectively. Thus, the carbonylic oxygen of (*S*)-zacopride forms a specific hydrogen bond with the active $g+$ rotamer of Thr3.36 (Fig. 5B), whereas the carbonylic oxygen of BIMU8 forms the hydrogen bond interaction with the active t rotamer of Trp6.48 (Fig. 5C). Accordingly, the T3.36A mutation almost abolished the benzamide and arylketone-induced 5-HT$_4$R stimulation (Fig. 3 and Table 1). We propose that benzamides and aryl ketones stabilize an R* state (R*-benzamides) by triggering the direct conforma-

tional transition of Thr3.36 (from the inactive $g-$ to the $g+$ conformation) by forming a specific hydrogen bond with Thr3.36.

The R*-BIMU8 State Is Primarily Reached after a Direct Interaction of Benzimidazolones with Trp6.48 and Triggering Its Toggle Switch from the *g*+ to *t* Conformation. The computational simulation presented above suggests that BIMU8 may trigger the process of 5-HT$_4$R activation (stabilization of the R*-BIMU8) mainly via the conformational transition of Trp6.48 from the $g+$ to the t conformation by a specific hydrogen bond interaction. To test this hypothesis, we analyzed the ability of BIMU8 to stimulate the W6.48A mutant. To our surprise, the K_D value for BIMU8 was unchanged (Table 1), whereas this mutation reduced the EC_{50} by 43-fold (Fig. 6B) and the E_{max} by a factor of 2 compared with 5-HT stimulation (Fig. 6A). This reduction of the BIMU8 stimulation was independent of the receptor density (Fig. 6B). The effects of T3.36A and W6.48A mutations in BIMU8 function suggest that the Thr3.36 toggle switch plays a minor role in the stabilization of R*-BIMU8 (E_{max} decreased from 97 to 78%), leaving the Trp6.48 toggle switch as the main mechanism of 5-HT$_4$R activation by BIMU8 (E_{max} decreased from 97 to 53%). We tried to generate the double T3.36A-W6.48A mutant receptor to fully impair the R*-BIMU8 state. Unfortunately, this double mutant receptor was poorly expressed at the cell surface, and no conclusion can be drawn.

Molecular models showed that in the absence of Trp6.48 (W6.48A mutant), the aromatic ring of BIMU8 can occupy the position of the active t conformation of Trp6.48 in the WT receptor (Fig. 6C). This position of the aromatic ring of BIMU8 in the receptor is very favorable because of the presence of the Phe5.47 aromatic side chain. In this new mode of binding, the carbonylic oxygen of BIMU8 forms a hydrogen bond interaction with the active $g+$ rotamer of Thr3.36 (Fig. 6C). It is likely that, in the W6.48A mutant receptor, the new R*-BIMU8 state is stabilized by this hydrogen bond, a mechanism of triggering an R* state similar to that of R*-benzamides (compare Fig. 5, B and C). This mode of binding explains why BIMU8 has similar binding affinity for WT and W6.48A mutant 5-HT$_4$R. Nevertheless, the lack of expression of this double T3.36A-W6.48A mutant receptor impedes an experimental probe of this hypothesis.

Discussion

One of the most important progresses in family A GPCR molecular pharmacology has been to understand, based on biophysical, biochemical, and crystallography experiments, how a multitude of chemically different agonists, which do not share a common binding mode, can trigger receptor activation. A few conserved molecular activation mechanisms implying the rearrangement of the side chains of a limited number of residues have been associated with receptor activation (Kobilka, 2007; Smit et al., 2007). A key question is to determine which different rearrangements of a given GPCR lead to the different R* states. Are they different for basal constitutively active R* and agonist-induced R* states? Do chemically different agonists induce different rearrangement? Few examples indicate that this could be the case. In the β_2-adrenergic receptor, salbutamol, although being an agonist, does not trigger the TM6 toggle switch, whereas the catechol derivatives do (Swaminath et al., 2004).

Here, we show that the R*basal of the WT 5-HT$_4$ receptor is likely to be the result of a simultaneous double toggle switch. One is the conformational change of Trp6.48 from the inactive $g+$ (pointing toward TM7) to the active t (TM5) conformation, which is accompanied by the conformational transition of Thr3.36 from the inactive $g-$ (TM6) to the active $g+$ (TM7) conformation. Both coordinated switches are necessary to go from the silent Rg to the R*basal. Indeed, mutation of either Trp6.48 or Thr3.36 to alanine kept the WT 5-HT$_4$ receptor to the Rg state whatever the receptor density. This Rg state was, of course, insensitive to inverse agonists. When the receptor is under the Rg state, the levels of cAMP accumulation were close to those observed in the absence of receptors (the mock-transfected cells). The Rg state is not often described in GPCR pharmacology (Joubert et al., 2002). The Rg state of rhodopsin is stabilized by the full inverse agonist *cis*-retinal, the structure of which is distinct from the ligand-free opsin state R (Lin and Sakmar, 1996; Park et al., 2008).

We have also shown that Thr3.36, in addition to modulating the Rg to R*basal, plays a minor role in the stabilization of R*-5-HT and R*-BIMU8 and is fully required in the stabilization of the R*-benzamides [(*S*)-zacopride, cisapride, and RS 67333]. Benzamides were completely inactive on the T3.36A mutant, whatever the receptor density, excluding a simple reduction in the coupling efficiency affecting prefer-

TABLE 1

Pharmacological properties of a series of 5-HT$_4$R ligands on WT 5HT$_4$R, T3.36A, and W6.48A mutant receptors

Binding assays were performed by using [^{3}H]GR 113808 as the specific 5-HT$_4$R radioligand in COS-7 cell membranes expressing either WT 5-HT$_4$R, 5-HT$_4$-T3.36A, or 5-HT$_4$-W6.48A. Nonspecific binding was determined with BIMU8 (10 μM). K_D values were determined from Cheng-Prusoff equation (Cheng and Prusoff, 1973). The agonist activity or potency (EC_{50}) was accessed as the concentration that gave 50% increase in the response to cAMP formation. The maximal activity of each drug (E_{max}) is expressed as a percentage of the maximum 5-HT response obtained with the WT at similar receptor density. All of the data are expressed as means ± S.E.M. of at least four separate experiments.

	WT			T3.36A			W6.48A		
	K_D	EC_{50}	E_{max}	K_D	EC_{50}	E_{max}	K_D	EC_{50}	E_{max}
	nM	*nM*	%	*nM*	*nM*	%	*nM*	*nM*	%
5-HT	77 ± 14	3.6 ± 0.7	100	1400 ± 2300	86 ± 33	74 ± 1	74 ± 26	89 ± 32	100
BIMU8	53 ± 12	18 ± 7	97 ± 4	210 ± 10	77 ± 17	78 ± 2	110 ± 70	540 ± 190	53 ± 3
(*S*)-Zacopride	640 ± 90	110 ± 20	77 ± 1	720 ± 150	N.D.	N.D.			
Cisapride	200 ± 20	43 ± 31	64 ± 1	730 ± 140	N.D.	N.D.			
RS 67333	5.5 ± 0.2	2.6 ± 1.5	70 ± 2	12 ± 3	N.D.	N.D.			

N.D., not determined.

entially the response to partial agonists such as benzamides. Thus, as a hypothesis, we can conclude that (*S*)-zacopride, cisapride, and RS 67333 trigger 5-HT$_4$R activation via stabilization of the rotamer toggle switch of Thr3.36 from the inactive *g*− to the active *g*+ conformation. Here, we show for the first time that the 3.36 position is directly implicated in agonist-induced activation and is responsible for the stabilization of an active state.

The 5-HT$_4$R is also activated by benzimidazolone ligands such as BIMU8. We propose that the R*-BIMU8 state is primarily reached after a direct interaction between the carbonylic oxygen of benzimidazolones and Trp6.48, triggering its toggle switch from the inactive *g*+ to the active *t* conformation. A similar mode of interaction between the Trp6.48 residue and the CSP-2503 agonist has been proposed during activation of the 5-HT$_{1A}$ receptors (Lopez-Rodriguez et al., 2005).

It was surprising that the W6.48A and T3.36A mutants were fully activated by 5-HT. This clearly indicates that the conformational mechanisms occurring from Rg to R*basal are different from those occurring from Rg to R*-5-HT. A two-state model was not sufficient to explain those results.

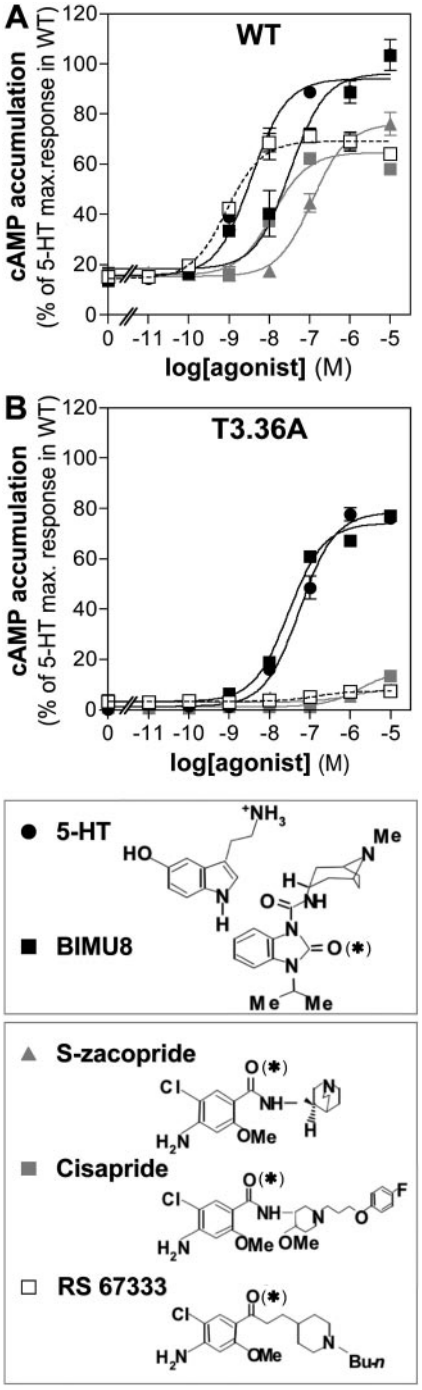

Fig. 3. Influence of Thr3.36 in the agonist-induced activation of the 5-HT$_4$R. Intracellular cAMP levels were measured in COS-7 cells transiently expressing 6160 and 5390 fmol/mg protein of WT 5-HT$_4$R (A) and T3.36A mutant receptor (B), respectively, in the presence of agonists belonging either to the indol (5-HT), benzamide [(*S*)-zacopride, cisapride], aryl ketone (RS 67333), or benzimidazolone (BIMU8) classes. Results are expressed as a percentage of the maximum cAMP production (8.9 ± 0.7 pmol/100,000 cells) induced by stimulating WT receptor with 5-HT (10^{-5} M). Each value represents the mean ± S.E.M. determined from three independent experiments performed in triplicate. Structures of the drugs used in the study are presented below the graph. Oxygen of the carbonyl group that interacts with either Thr3.36 or Trp6.48 is designated with an asterisk.

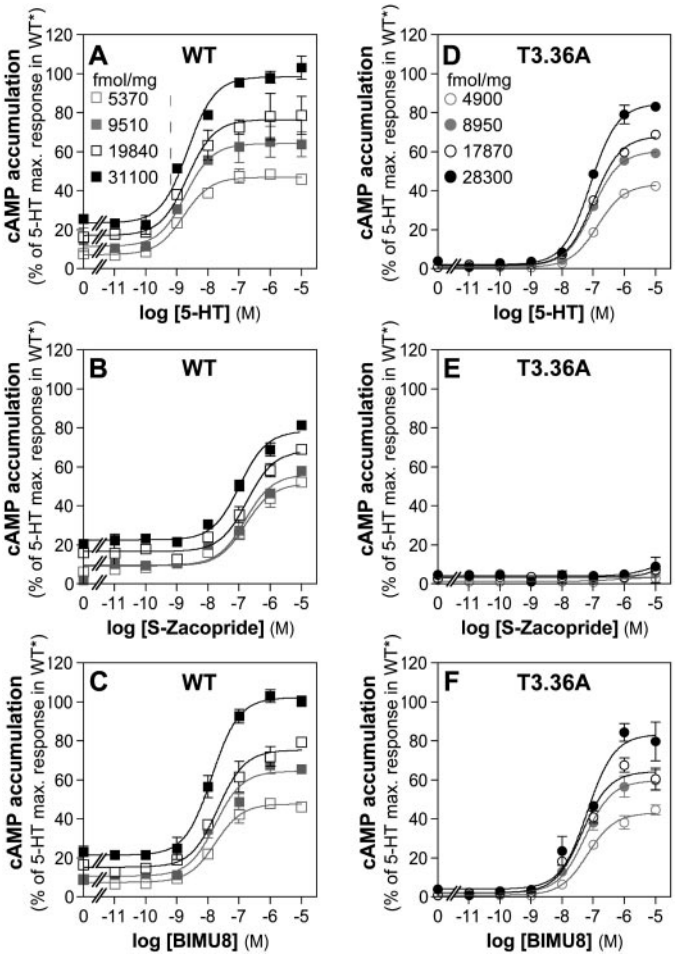

Fig. 4. Effect of increasing T3.36A receptor density on agonist activation. cAMP accumulation at different densities of WT (A–C) and T3.36A (D–F) 5-HT$_4$Rs, transiently expressed in COS-7 cells, was measured over 10-min stimulation induced by 5-HT (A and D), (*S*)-zacopride (B and E), or BIMU8 (C and F). *, data are expressed as a percentage of maximal stimulation due to 5-HT in WT expressing the highest receptor density (31,100 fmol/mg protein). COS-7 cells were transfected with increasing amount of DNA (50, 100, 200, and 500 ng) corresponding to 5370 ± 1830, 9510 ± 1070, 19840 ± 2300, and 31,100 ± 1600 fmol/mg protein for WT and 4900 ± 880, 8950 ± 130, 17,870 ± 750, and 28,300 ± 3950 fmol/mg of protein for T3.36A mutant.

The 5-HT_4Rs and rhodopsin are, at least, in equilibrium between three states (i.e., the Rg, the R*basal, and the R*-5-HT states). The R*-5-HT state can be reached either from the Rg or from the R*basal state. Thus, the relative stimulation by 5-HT was higher in cells expressing the receptor under the Rg state (W6.48A and T3.36A mutants) than under the R*basal state (WT receptors) (Fig. 1). A similar observation can be done considering the WT and the T3.36A mutant and the stimulation by BIMU8. The relative stimulation by BIMU8 was higher in cells expressing the T3.36A mutant (under the Rg state) than the WT receptors (under the R*basal state) (Fig. 3).

To date, there is not a clear idea as to the rearrangements occurring upon 5-HT stimulation. However, it has been shown for the β_2-adrenergic receptor, using fluorescence spectroscopy

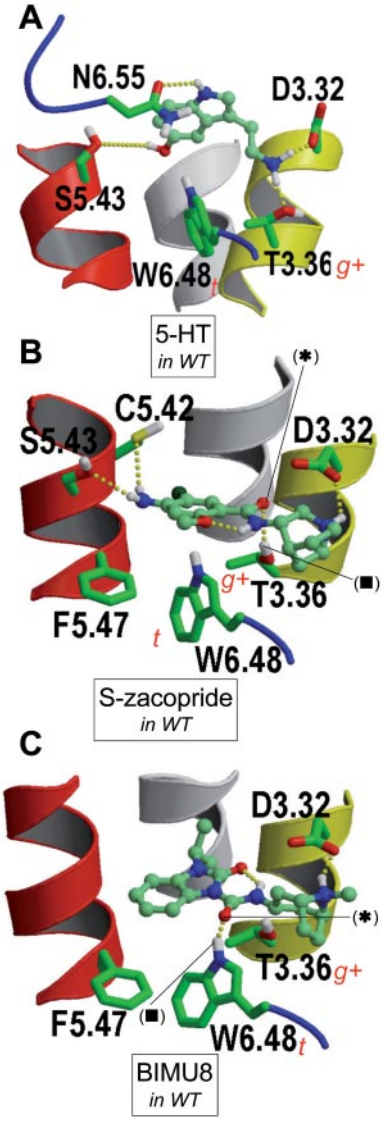

Fig. 5. Computational models of the complexes between 5-HT_4R and BIMU8 or zacopride. In these models, the protonated moiety of the ligands interact with Asp3.32; the 5-OH and NH moieties of 5-HT hydrogen bond the key Ser5.43 and Asn6.55 side chains (A) as proposed by site-directed mutagenesis (Mialet et al., 2000); the $-C(CH_3)_2$ and –Cl moieties of BIMU8 and (*S*)-zacopride, respectively, are located in a small hydrophobic cavity between TMs 3 to 5 (B and C) and the $-NH_2$ group of (*S*)-zacopride hydrogen bonds Ser5.43 (B). BIMU8 and (*S*)-zacopride form an intramolecular hydrogen bond between the –NH amide and a carbonyl or methoxy group, respectively. BIMU8 elicits 5-HT_4R activation by forming a hydrogen bond interaction with Trp6.48 in the active *t* conformation (C), whereas (*S*)-zacopride triggers activation via the interaction with Thr3.36 in the active *g*+ conformation (B). The atoms implicated in these interactions are indicated: oxygen of the drugs is marked with an asterisk, and Thr3.36 or Trp6.48 hydrogen is labeled with a closed square.

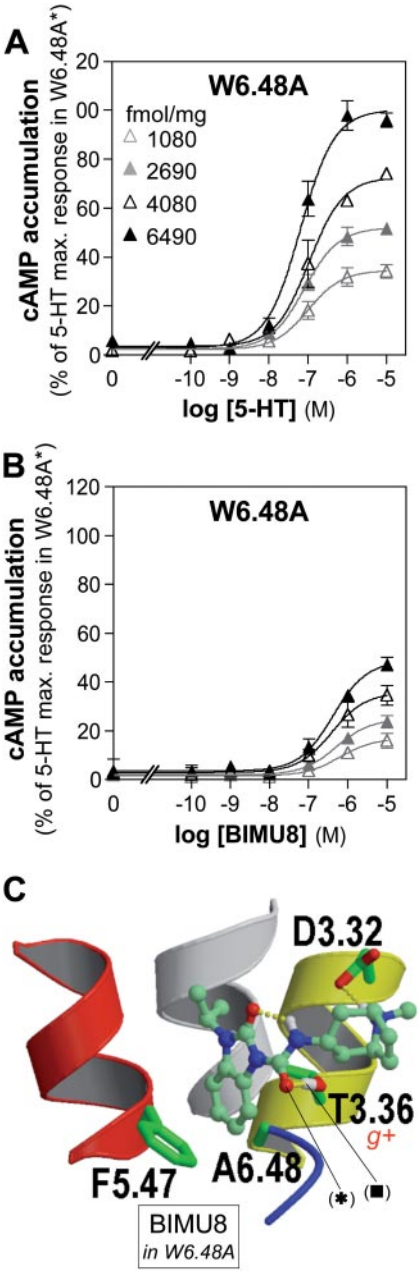

Fig. 6. Influence of Trp6.48 in the BIMU8-induced activation of the 5-HT_4R. cAMP accumulation at different densities of 5-HT_4-W6.48A mutant, transiently expressed in COS-7 cells, was measured over 10-min stimulation induced by 5-HT (A) or BIMU8 (B). *, data are expressed as a percentage of maximal stimulation due to 5-HT in W6.48A mutant expressing the highest receptor density (6490 fmol/mg protein). COS-7 cells were transfected with increasing amount of DNA (200, 500, 1000, and 2000 ng) corresponding to 1080 ± 260, 2690 ± 280, 4080 ± 880, and 6490 ± 520 fmol/mg protein of W6.48A mutant. C, computational models of the complex between BIMU8 and W6.48A mutant receptor. In the absence of Trp6.48, the aromatic ring of BIMU8 occupies the position of the active *t* conformation of Trp6.48 in the WT receptor (see Fig. 5C), and the carbonylic oxygen hydrogen bonds the active *g*+ rotamer of Thr3.36. The atoms implicated in this interaction are indicated: oxygen of the drug is marked with an asterisk, and Thr3.36 hydrogen is labeled with a closed square.

to monitor agonist-induced conformational changes, that relocation of the extracellular side of TM5 is necessary to facilitate binding of the catechol hydroxyls to the serine residues at positions 5.42 and 5.46 (Swaminath et al., 2004). In addition, TM6 performs an inward movement of the extracellular part toward TM3 (the global toggle switch of Schwartz et al., 2006) that is stabilized by the interaction with agonists. By homology with these proposals, we suggest that 5-HT would stabilize R*-5-HT by the interaction between the 5-OH and NH moieties with the Ser5.43 and Asn6.55 side chains, respectively, triggering the proposed movements of TMs 5 and 6.

The mechanisms by which binding of these chemical signals at the extracellular domain of the receptor trigger a set of conformational rearrangements of the TM segments near the G-protein binding domain are not fully understood. Nevertheless, comparison of the structure of inactive rhodopsin (Li et al., 2004) with the crystal structure of the ligand-free opsin (Park et al., 2008) has provided additional insights into these processes. Specifically, we propose that the Thr3.36/Trp6.48 rotamer toggle switch disrupts a conserved hydrogen bond network linking Trp6.48 and Asp2.50 (Li et al., 2004; Pardo et al., 2007; Rosenbaum et al., 2007), triggering the conformational transition of Asn7.49 toward Asp2.50 (Urizar et al., 2005) and ultimately leading to the extended conformation, pointing toward the protein core, of Arg3.50 (Park et al., 2008). On the other hand, the agonist-induced inward movement of the extracellular part of TM6 toward TM3 (Schwartz et al., 2006) might cause the intracellular movement of TM6 toward TM5, facilitating the observed ionic interaction between Glu6.30 and Lys5.66 (Park et al., 2008). Finally, the relocation of the extracellular side of TM5 to facilitate binding of biogenic amine agonists (Swaminath et al., 2004) induces the intracellular movement of TM5, enabling the interaction of Tyr5.58 with the extended conformation of Arg3.50 (Park et al., 2008).

We have previously established, using circular dichroism difference spectra of purified 5-HT$_4$R, that free (or neutral antagonist-occupied), agonist-occupied (partial or full agonist), and silent (inverse agonist-occupied) receptors involved different arrangements of the e2 loop (Baneres et al., 2005). Here, in a cellular context, we provide arguments in favor of different conformational arrangements during stabilization of different 5-HT$_4$ R* states: the R*basal, the R*-5-HT, the R*-benzamides, and the R*-BIMU8.

Acknowledgments

We are grateful to Angela Turner Madeuf for help in language revision and to Elisabeth Cassier for technical assistance.

References

Alves ID, Salamon Z, Varga E, Yamamura HI, Tollin G, and Hruby VJ (2003) Direct observation of G-protein binding to the human δ-opioid receptor using plasmon-waveguide resonance spectroscopy. *J Biol Chem* **278:**48890–48897.

Ansanay H, Sebben M, Bockaert J, and Dumuis A (1996) Pharmacological comparison between [^{3}H]-GR113808 binding sites and functional 5-HT$_4$ receptors in neurons. *Eur J Pharmacol* **298:**165–174.

Ballesteros J and Weinstein H (1995) Integrated methods for the construction of three dimensional models and computational probing of structure-function relations in G protein coupled receptors, in *Methods in Neurosciences* **25:**366–428.

Ballesteros JA, Deupi X, Olivella M, Haaksma EE, and Pardo L (2000) Serine and threonine residues bend alpha-helices in the chi(1) = g(−) conformation. *Biophys J* **79:**2754–2760.

Banères JL, Mesnier D, Martin A, Joubert L, Dumuis A, and Bockaert J (2005) Molecular characterization of a purified 5-HT4 receptor: a structural basis for drug efficacy. *J Biol Chem* **280:**20253–20260.

Barthet G, Gaven F, Framery B, Shinjo K, Nakamura T, Claeysen S, Bockaert J, and Dumuis A (2005) Uncoupling and endocytosis of 5-hydroxytryptamine 4 receptors. Distinct molecular events with different GRK2 requirements. *J Biol Chem* **280:**27924–27934.

Bond RA, Leff P, Johnson TD, Milano CA, Rockman HA, McMinn TR, Apparsundaram S, Hyek MF, Kenakin TP, and Allen LF (1995) Physiological effects of inverse agonists in transgenic mice with myocardial overexpression of the beta 2-adrenoceptor. *Nature* **374:**272–276.

Case D, Darden T, Cheatham T, Simmerling C, and Wang J (2006) AMBER 9, University of California, San Francisco, CA.

Cheng Y and Prusoff WH (1973) Relationship between the inhibition constant (K1) and the concentration of inhibitor which causes 50 per cent inhibition (I50) of an enzymatic reaction. *Biochem Pharmacol* **22:**3099–3108.

Cherezov V, Rosenbaum DM, Hanson MA, Rasmussen SG, Thian FS, Kobilka TS, Choi HJ, Kuhn P, Weis WI, Kobilka BK, et al. (2007) High-resolution crystal structure of an engineered human beta2-adrenergic G protein-coupled receptor. *Science* **318:**1258–1265.

Claeysen S, Joubert L, Sebben M, Bockaert J, and Dumuis A (2003) A single mutation in the 5-HT4 receptor (5-HT4-R D100(3.32)A) generates a Gs-coupled receptor activated exclusively by synthetic ligands (RASSL). *J Biol Chem* **278:**699–702.

Claeysen S, Sebben M, Becamel C, Bockaert J, and Dumuis A (1999) Novel brain-specific 5-HT4 receptor splice variants show marked constitutive activity: role of the C-terminal intracellular domain. *Mol Pharmacol* **55:**910–920.

Claeysen S, Sebben M, Bécamel C, Eglen RM, Clark RD, Bockaert J, and Dumuis A (2000) Pharmacological properties of 5-hydroxytryptamine$_4$ receptor antagonists on constitutively active wild-type and mutated receptors. *Mol Pharmacol* **58:**136–144.

Duan Y, Wu C, Chowdhury S, Lee MC, Xiong G, Zhang W, Yang R, Cieplak P, Luo R, Lee T, et al. (2003) A point-charge force field for molecular mechanics simulations of proteins based on condensed-phase quantum mechanical calculations. *J Comput Chem* **24:**1999–2012.

Ghanouni P, Gryczynski Z, Steenhuis JJ, Lee TW, Farrens DL, Lakowicz JR, and Kobilka BK (2001) Functionally different agonists induce distinct conformations in the G protein coupling domain of the β2 adrenergic receptor. *J Biol Chem* **276:**24433–24436.

Jongejan A, Bruysters M, Ballesteros JA, Haaksma E, Bakker RA, Pardo L, and Leurs R (2005) Linking agonist binding to histamine H1 receptor activation. *Nat Chem Biol* **1:**98–103.

Joubert L, Claeysen S, Sebben M, Bessis AS, Clark RD, Martin RS, Bockaert J, and Dumuis A (2002) A 5-HT4 receptor transmembrane network implicated in the activity of inverse agonists but not agonists. *J Biol Chem* **277:**25502–25511.

Kobilka BK (2007) G protein coupled receptor structure and activation. *Biochim Biophys Acta* **1768:**794–807.

Leff P (1995) The two-state model of receptor activation. *Trends Pharmacol Sci* **16:**89–97.

Li J, Edwards PC, Burghammer M, Villa C, and Schertler GF (2004) Structure of bovine rhodopsin in a trigonal crystal form. *J Mol Biol* **343:**1409–1438.

Lin SW and Sakmar TP (1996) Specific tryptophan UV-absorbance changes are probes of the transition of rhodopsin to its active state. *Biochemistry* **35:**11149–11159.

López-Rodríguez ML, Morcillo MJ, Fernández E, Benhamú B, Tejada I, Ayala D, Viso A, Campillo M, Pardo L, Delgado M, et al. (2005) Synthesis and structure-activity relationships of a new model of arylpiperazines. 8. Computational simulation of ligand-receptor interaction of 5-HT(1A)R agonists with selectivity over alpha1-adrenoceptors. *J Med Chem* **48:**2548–2558.

McAllister SD, Hurst DP, Barnett-Norris J, Lynch D, Reggio PH, and Abood ME (2004) Structural mimicry in class A G protein-coupled receptor rotamer toggle switches: the importance of the F3.36(201)/W6.48(357) interaction in cannabinoid CB1 receptor activation. *J Biol Chem* **279:**48024–48037.

McGregor MJ, Islam SA, and Sternberg MJ (1987) Analysis of the relationship between side-chain conformation and secondary structure in globular proteins. *J Mol Biol* **198:**295–310.

Mialet J, Dahmoune Y, Lezoualc'h F, Berque-Bestel I, Eftekhari P, Hoebeke J, Sicsic S, Langlois M, and Fischmeister R (2000) Exploration of the ligand binding site of the human 5-HT(4) receptor by site-directed mutagenesis and molecular modeling. *Br J Pharmacol* **130:**527–538.

Okada T, Ernst OP, Palczewski K, and Hofmann KP (2001) Activation of rhodopsin: new insights from structural and biochemical studies. *Trends Biochem Sci* **26:**318–324.

Palczewski K, Kumasaka T, Hori T, Behnke CA, Motoshima H, Fox BA, Le Trong I, Teller DC, Okada T, Stenkamp RE, et al. (2000) Crystal structure of rhodopsin: a G protein-coupled receptor. *Science* **289:**739–745.

Pardo L, Deupi X, Dölker N, López-Rodríguez ML, and Campillo M (2007) The role of internal water molecules in the structure and function of the rhodopsin family of G protein-coupled receptors. *Chembiochem* **8:**19–24.

Park JH, Scheerer P, Hofmann KP, Choe HW, and Ernst OP (2008) Crystal structure of the ligand-free G-protein-coupled receptor opsin. *Nature* **454:**183–187.

Rosenbaum DM, Cherezov V, Hanson MA, Rasmussen SG, Thian FS, Kobilka TS, Choi HJ, Yao XJ, Weis WI, Stevens RC, et al. (2007) GPCR engineering yields high-resolution structural insights into beta2-adrenergic receptor function. *Science* **318:**1266–1273.

Ruprecht JJ, Mielke T, Vogel R, Villa C, and Schertler GF (2004) Electron crystallography reveals the structure of metarhodopsin I. *EMBO J* **23:**3609–3620.

Samama P, Cotecchia S, Costa T, and Lefkowitz RJ (1993) A mutation-induced activated state of the β_2-adrenergic receptor. Extending the ternary complex model. *J Biol Chem* **268:**4625–4636.

Schertler GF (2005) Structure of rhodopsin and the metarhodopsin I photointermediate. *Curr Opin Struct Biol* **15:**408–415.

Schwartz TW, Frimurer TM, Holst B, Rosenkilde MM, and Elling CE (2006) Molecular mechanism of 7TM receptor activation—a global toggle switch model. *Annu Rev Pharmacol Toxicol* **46:**481–519.

Shi L and Javitch JA (2002) The binding site of aminergic G protein-coupled receptors: the transmembrane segments and second extracellular loop. *Annu Rev Pharmacol Toxicol* **42:**437–467.
Shi L, Liapakis G, Xu R, Guarnieri F, Ballesteros JA, and Javitch JA (2002) β2 Adrenergic receptor activation. Modulation of the proline kink in transmembrane 6 by a rotamer toggle switch. *J Biol Chem* **277:**40989–40996.
Smit MJ, Vischer HF, Bakker RA, Jongejan A, Timmerman H, Pardo L, and Leurs R (2007) Pharmacogenomic and structural analysis of constitutive g protein-coupled receptor activity. *Annu Rev Pharmacol Toxicol* **47:**53–87.
Swaminath G, Xiang Y, Lee TW, Steenhuis J, Parnot C, and Kobilka BK (2004) Sequential binding of agonists to the β2 adrenoceptor. Kinetic evidence for intermediate conformational states. *J Biol Chem* **279:**686–691.
Urizar E, Claeysen S, Deupí X, Govaerts C, Costagliola S, Vassart G, and Pardo L (2005) An activation switch in the rhodopsin family of G protein-coupled receptors: the thyrotropin receptor. *J Biol Chem* **280:**17135–17141.
Visiers I, Ballesteros JA, and Weinstein H (2002) Three-dimensional representations of G protein-coupled receptor structures and mechanisms. *Methods Enzymol* **343:** 329–371.
Wang J, Wolf RM, Caldwell JW, Kollman PA, and Case DA (2004) Development and testing of a general amber force field. *J Comput Chem* **25:**1157–1174.

Address correspondence to: Dr. Joël Bockaert, Institut de Génomique Fonctionnelle, 141 Rue de la Cardonille, 34094 Montpellier Cedex 5, France. E-mail: joel.bockaert@igf.cnrs.fr